Dalton Transactions

This article can be cited before page numbers have been issued, to do this please use: A. Meduri, M. Cozzolino, S. Milione, K. Press, E. Sergeeva, C. Tedesco, M. Mazzeo and M. Lamberti, *Dalton Trans.*, 2015, DOI: 10.1039/C5DT02938D.

www.rsc.org/dalton

View Article Online
DOI: 10.1039/C5DT02938D

Journal Name

ARTICLE

Yttrium and Aluminium Complexes bearing Dithiodiolate Ligands: Synthesis and Application in Cyclic Esters Polymerization

Received 00th January 20xx,
Accepted 00th January 20xx

DOI: 10.1039/x0xx00000x

www.rsc.org/

A. Meduri,[a] M. Cozzolino,[a] S. Milione,[a] K. Press,[b] E. Sergeeva,[b] C. Tedesco,[a] M. Mazzeo[a] and M. Lamberti[c,]*

Yttrium and aluminium complexes of two dithiodiolate ligands that feature different bridges $(CF_3)_2C(OH)CH_2SRSCH_2C(OH)(CF_3)_2$ (L^1-H_2, R = CH_2CH_2 and L^2-H_2, R = C_6H_4), were synthesized in good yields by reacting tris(silylamide)yttrium or trimethylaluminium with one equivalent of the proligand. All complexes were characterized by NMR and elemental analysis, single-crystal X-ray structural analysis was also performed for one of the yttrium complexes. The catalytic activities of the four complexes in the ring-opening polymerization of ε-caprolactone and *rac*-lactide have been investigated. Furthermore, DOSY experiment and DFT calculations have been carried out to clarify the structure of the isopropoxo derivative of the complex L^2Yamide.

Introduction

Ring-opening polymerization (ROP) of cyclic esters promoted by metal catalysts has emerged as the most promising route for the synthesis of aliphatic polyesters, such as poly-caprolactone and polylactide, with tuned properties.[1] Taking into account the importance of such class of polymers in several fields (packaging, agricultural and biomedical areas[2]) numerous researches have focused on the exploration of new metal complexes that are active in the ROP of cyclic esters. Among the most successful catalysts, yttrium complexes have emerged for their high activity and good polymerization control,[1,3] whereas aluminium complexes have played a special role thanks to the high degree of stereocontrol which they are able to induce,[4] allowing, for example, the preparation of new polylactide (PLA) microstructures.[5] Moreover, both these metals are non toxic so that the synthesized polyesters can be employed for any use, from the food industry to the biomedical field,[1a] with no concern about possible catalyst residue. The choice of the ancillary ligand is another crucial aspect in the design of an efficient catalytic system. Numerous new ligands have been prepared allowing detailed studies of the effect of the coordinative environments on the catalytic properties of the synthesized complexes. In particular, while the use of ancillary ligands bearing phenoxy groups as anionic donors and nitrogen atoms as neutral donors has been ubiquitous, alkoxide anionic donors and sulphur neutral donors have been much less explored.[6] Carpentier has developed aluminium complexes bearing fluorinated (di)alkoxy-diimino ligands that show comparable efficiency as ROP catalysts to their aryloxide analogues.[7] A series of 1,ω-dithiaalkanediyl-bridged bis(phenol)s (OSSO) have been introduced by Okuda as ancillary ligands for third group metal complexes. By variation of the ligand architecture, moderate to high heteroselectivity for the ROP of *rac*-LA has been obtained.[8] For these systems, the ligand fluxionality resulted crucial in the mechanism of stereoselection. Following these remarkable results we subsequently explored the behaviour of a series of metal complexes bearing the unbridged bidentate phenoxythioether (OS) ligands in the ROP of cyclic esters.[6c,9]
Some of us recently reported, for the first time, a new class of ligands: the dithiodiolate ligands, bearing both alkoxide anionic donors and sulphur neutral donors in the same skeleton. Interestingly, dithiodiolate Group 4 complexes resulted highly active catalysts for the production of heterotactic PLAs.[10] In this framework, we decided to explore the coordination chemistry of dithiodiolate ligands around other metals, focusing our attention on yttrium and aluminium, and to test the synthesized complexes as catalysts in the ROP of ε-caprolactone and lactides.

Results and discussion

Synthesis and characterization of yttrium and aluminium complexes 1-4

---

[a] Dipartimento di Chimica e Biologia, Università di Salerno, via Giovanni Paolo II 132, I-84084, Fisciano, Salerno, Italy.
[b] School of Chemistry, Raymond and Beverly Sackler Faculty of Exact Sciences, Tel Aviv University, Ramat Aviv, Tel Aviv 69978, Israel
[c] Dipartimento di Fisica "E. Caianiello", Università di Salerno, via Giovanni Paolo II 132, I-84084, Fi-sciano, Salerno, Italy

Electronic Supplementary Information (ESI) available: NMR characterization, kinetics data and tetrad distribution analysis. CCDC 1405712 contains the crystallographic data. See DOI: 10.1039/x0xx00000x

View Article Online
DOI: 10.1039/C5DT02938D

Yttrium complexes **1** and **2** were prepared by the amine elimination reactions between the silyl amido precursor {$Y[N(SiHMe_2)_2]_3(THF)_2$} and the proligands L^1-H_2 and L^2-H_2, (see Scheme 1) at room temperature in benzene solution. In both cases the corresponding monosilylamido complexes $L^1Y[N(SiHMe_2)_2](THF)$ **1** and $L^2Y[N(SiHMe_2)_2](THF)$ **2** were obtained in high yield (92% and 89%, respectively).

An NMR-scale reaction of yttrium silylamide {$Y[N(SiHMe_2)_2]_3(THF)$} with one equiv of L^1-H_2 was carried out in benzene-d_6 at room temperature. A quantitative complexation was observed after 4 h. Solution ^1H NMR studies of the reaction indicated that the neutral proligand was deprotonated by two metal silylamide groups of {$Y[N(SiHMe_2)_2]_3(THF)$} with the release of 2 equiv of bis(dimethylsilyl)amine (Scheme 1).

^1H, ^{19}F and ^{13}C NMR spectra at room temperature of complex **1** showed a single set of resonances indicative of the presence of a single isomer on the NMR time scale. The sulphur coordination binding to the central yttrium metal was confirmed by the slight downfield shift of the SCH_2-$C(CF_3)_2$ protons (2.9 ppm) compared to the corresponding diol proligand (2.6 ppm). The silylamide group displayed a single doublet for the four equivalent methyl groups and one septet for Si-H protons. The resonance relative to the α-CH_2 protons of the THF molecule (at 3.90 ppm) shifted downfield with respect to the free THF (3.57 ppm) suggesting the coordination of the THF at the metal centre.[8b] NMR data for complex **1** were coherent with a structure consisting of one ligand, one amide group and one THF molecule coordinated at the metal centre. For the equivalent protons of the two methylene groups CH_2-S of the ethylene bridge, a single sharp signal was observed. Analogously, ^{19}F NMR spectrum contained only one sharp signal, indicating that all four CF_3 groups in the complex are equivalent. This picture is indicative either of the presence of a highly symmetric structure or the existence of a fast fluxional process on the NMR time scale. Actually, the methylene protons of the SCH_2-$C(CF_3)_2$ groups appeared in the ^1H NMR spectrum as a broad signal, suggesting the existence of an averaging process in solution. This broad resonance sharpened on heating to 323 K and, at this temperature, the spectrum showed all resonances as sharp signals. On the other hand, at low temperature (203 K) the four protons of the SCH_2-$C(CF_3)_2$ groups resolved into two doublets. This aspect was carefully studied by NMR variable temperature experiments (vide infra).

Analogously to complex **1**, for complex **2** the NMR data suggested the formation of a single isomer with a structure consisting of one ligand, one amide group and one THF molecule coordinated at the metal centre.

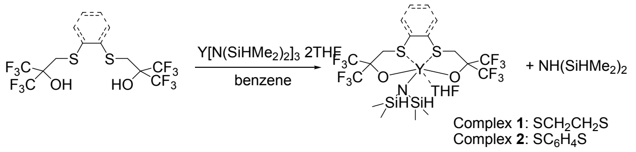

Scheme 1. Synthetic pathway for the synthesis of complexes **1**-**2**

In this case, the SCH_2-$C(CF_3)_2$ protons were observed at 3.40 ppm (cfr with 3.08 ppm value observed for the same protons of the corresponding diol proligand) and appeared as a narrow peak. The α-CH_2 protons of the THF molecule were observed at 3.93 ppm.

X-ray diffraction quality single crystals of **2** were obtained as yellow prisms from hexane solutions at 253K. The X-ray molecular structure is shown in Figure 1, selected bond distances and angles are listed in Table S1. The yttrium atom is six-coordinate, adopting a distorted trigonal-prismatic geometry, where the two oxygen donors of the dithiodiolate ligand are cis-oriented, as indicated by O1-Y1-O2 angle of 109.26(19)°, and also the nitrogen and THF oxygen atoms are cis-oriented (N1-Y1-O3 91.26(19)°). The same configuration was also found in yttrium complexes bearing a salen[11] or a dithiodiphenolate ligand.[12] Y1-O1 and Y-O2 distances are respectively 2.153(5) Å and 2.122(5) Å, and Y-S1 and Y-S2 distances are respectively 2.948(2) Å and 2.973(2) Å, similar values have been observed in analogous six-coordinate Y complexes.[11,12] The Y atom results to be displaced by 1.05 Å from the mean plane (rmsd 0.195 Å) formed by O1, O2, S1 and S2 atoms of the chelating ligand, almost the same value is observed for the dithiophenolate Y complex (1.08 Å) and a slightly lower value (0.95 Å) for the salen Y complex.

Y1-Si1 and Y1-Si2 contacts are 3.229(3) Å and 3.480(3) Å, the former distance displays a shorter value than those observed for the analogous Y dithiophenolate complex (3.338 Å and 3.318 Å), where the presence of a β(Si-H) agostic interaction was excluded.‡

To investigate the structures of complexes **1** and **2** in solution, variable-temperature ^1H NMR spectra in toluene-d_8 were recorded. When tetradentate ligands, as the OSSO diolate ligands, wrap around six coordinate metal centre in an octahedral fashion, three geometries are possible, designated as *mer-mer* (*trans*), *fac-fac* (*cis*-α), or *fac-mer* (*cis*-β). Taking into account that sulphur donors become stereogenic upon binding to the metal and that two different labile ligands (amide and THF) are coordinated to the metal centre, all the

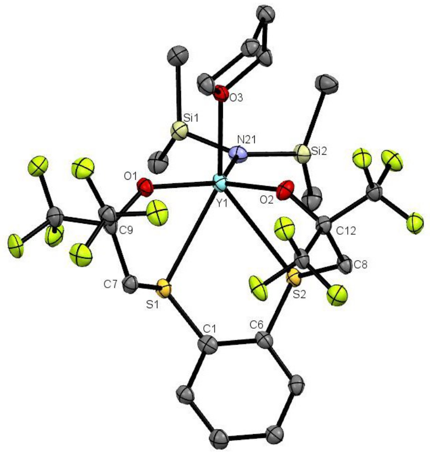

Figure 1. ORTEP drawing of compound **2**. Hydrogen atoms have been omitted for clarity. Ellipsoids are drawn at 30% probability level.

View Article Online
DOI: 10.1039/C5DT02938D

possible isomers are C_1 symmetric, except for the *trans* isomers in which the sulphur atoms have opposite configuration (Scheme 2).[13]

However, as already discussed, the broadness of the observed signals at room temperature indicates a fluxional behaviour of complexes **1** and **2** in solution.

The VT NMR analysis of complex **1** (Figure 2) showed that, at sub-ambient temperature, the two methylene protons S-CH$_2$-C(CF$_3$)$_2$ resolve into a diastereotopic AB pattern ($^2J_{HH}$ = 13 Hz). The coalescence of the signals was observed at 283 K; below this temperature the resonances became sharp and well resolved. Kinetic parameters were calculated using line-shape analysis of the ^{1}H NMR data over the temperature range (193 - 338 K). The activation enthalpy ($\Delta H^{\#}$= 1.84 Kcal/mol) and entropy ($\Delta S^{\#}$= -40.24 cal/mol K) values were evaluated from the Eyring plot (Figure S9, Supporting Information). The negative entropy of activation suggests that rearrangement of the ligands occurs via a non-dissociative mechanism, indicating strong metal–sulphur bonds.

The whole picture demonstrates the presence in solution of a symmetric isomer (C_2 or C_S), signifying either the formation of the C_S-symmetric octahedral isomer with *trans* geometry (all the other possible octahedral isomers have lower symmetry), or the presence of a species with a trigonal-prismatic geometry, i.e. the solid state structure is retained in solution. § In both cases one single species is present in solution and the observed fluxionality may be due to fast conformation change of the six-membered-ring yttrium metallacycles.

At 298 K, the ^{1}H NMR spectrum of complex **2** showed narrow peaks. Upon lowering the temperature to 208 K, the S-CH$_2$-C(CF$_3$)$_2$ methylene protons were resolved into two sets of signals, at least. The main signal (70 %) appeared as a broad signal, while minor signals appeared as an AB pattern consistent with C_2 or C_S symmetry. These spectra were reversibly reproduced over the temperature range examined, indicating a reversible fluxional process between several isomers.

The reactions of the proligands L^1-H$_2$ and L^2-H$_2$ with 1 equiv of the aluminium precursor AlMe$_3$ took place immediately on addition at room temperature in benzene (Scheme 3). The reaction mixtures were kept stirring for 1 h to afford the aluminium methyl complexes **3** and **4** in good yields (73% and 87%, respectively).

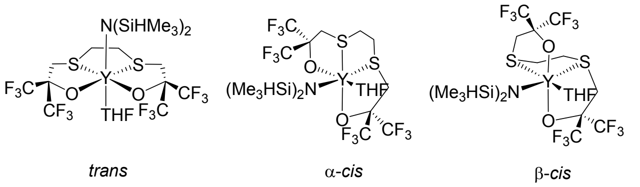

Scheme 2. Representative isomers for the octahedral (OSSO)Y[N(SiHMe$_2$)$_2$](THF) complexes. All the other possible isomers can be obtained taking into account both the chirality of the sulphur atoms and the interchange of the two labile ligands.

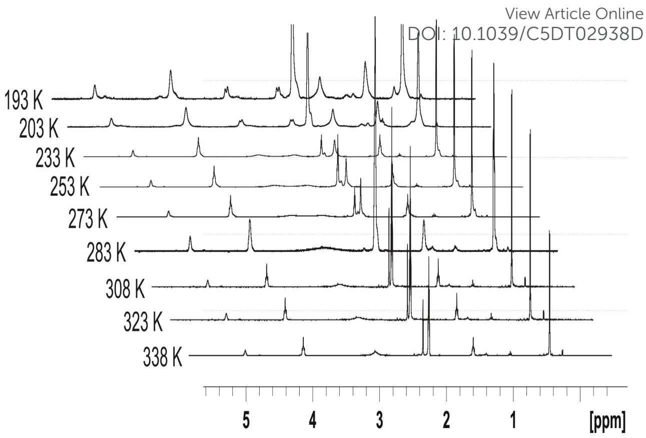

Figure 2. Variable-temperature ^{1}H NMR spectra of **1** in toluene-d$_8$.

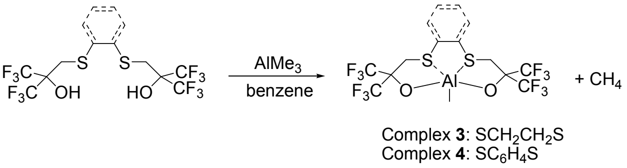

Scheme 3. Synthetic pathway for the synthesis of complexes **3**-**4**.

NMR studies of the reactions performed in benzene-d$_6$ indicated that the neutral proligands were deprotonated by two alkyls of trimethylaluminium with the release of 2 equiv of methane. The disappearance of the O-H signal of the free ligands and the appearance of a resonance for the protons of the methyl bound to the aluminium in the highfield region of the ^{1}H NMR spectra (-0.13 and -0.08 ppm for complexes **3** and **4**, respectively) demonstrated the formation of the desired complexes. In particular, for complex **4** the two methylene protons S-CH$_2$-C(CF$_3$)$_2$ resulted diastereotopic, appearing as an AB-system. This demonstrates both the coordination of the ligand in a tetradentate fashion and the formation of a C_2- or a C_S-symmetric isomer.

On the other hand for complex **3** the analogous methylene S-CH$_2$-C(CF$_3$)$_2$ protons appeared, at room temperature, as a broad signal. In this case, a well resolved AB-system for these protons was observed in the ^{1}H NMR spectrum acquired at 233 K (see the Supporting Information).

The higher rigidity of the phenylene group, with respect to that of the ethylene group, can determine a stronger coordination of the sulphur atoms to the aluminium centre in complex **4**, and so explain its lower fluxionality with respect to that of complex **3**.

The ^{19}F NMR spectrum of **3** displayed a broad signal. For complex **4** two sharp quartets of equal intensity were observed, indicating that the two CF$_3$ groups within each C(CF$_3$)$_2$ moiety are magnetically nonequivalent, coherently with the symmetry deduced by the ^{1}H NMR spectrum.

Ring-opening polymerization of ε-caprolactone and *rac*-lactide by catalysts 1 and 2.

The prepared yttrium-amide complexes were investigated in the ROP of ε-caprolactone.

Representative data from a series of polymerizations conducted in toluene are collected in Table 1. The polymers, precipitated from the reaction medium by addition of wet hexane, were analyzed by NMR spectroscopy and gel permeation chromatography (GPC).

Under mild reaction conditions, complexes **1** and **2** alone exhibited extremely high activity with turnover frequency among the highest reported in literature (TOF up to 1.2 10^5 h^{-1}). The high productivity was also preserved when a low catalyst loading (2 μmol) and high monomer/initiator molar ratio were employed (run 3, Table 1). Under the reaction conditions explored, complex **2** showed higher catalytic activity than complex **1** (runs 1 and 2, Table 1).

The GPC analyses of the polymers showed monomodal distributions of the molecular weights and polydispersity indexes relatively broad ($1.60 \leq M_w/M_n \leq 2.1$). However, the number-average molecular weights (M_n,GPC, Table 1) were higher than those calculated on the assumption that a single polymeric chain was produced per metal centre. This observation suggests that only a percentage of metal centres is involved in the catalytic process. One of the most common reason is a low initiation efficiency by the leaving group because of its low nucleophilicity.[15,9a] To verify this hypothesis, additional polymerization reactions were performed in the presence of isopropanol. The addition of an external alcohol is a common expedient to introduce highly reactive initiation groups such as alkoxides on the metal centre. This allows the production of polymeric chains of predictable molecular weights and narrow molecular weight distributions. After the addition of 1 equiv. of isopropanol as a co-initiator, the catalytic activity of the amide precursors **1** and **2** drastically decreased.

After 30 minutes, at room temperature, the monomer conversion was lower than 10%. Probably, the formation of dimeric yttrium alkoxo species was responsible for the drop of activity.

Table 1. Polymerization of ε-caprolactone by catalysts **1**-**2**.[a]

Run	cat	^{i}PrOH (eq)	T (°C)	t (min)	conv[b] (%)	$M_{n,th}$[c] (kDa)	$M_{n,GPC}$[d] (kDa)	M_w/M_n[d]
1	1	-	25	2	82	47.7	209.4	1.60
2	2	-	25	0.25	100	57.1	181.6	2.11
3[e]	2	-	25	5	81	92.4	328.9	1.82
4[f]	1	1	70	30	98	55.9	40.2	1.27
5[g]	1	2	70	30	90	25.6	20.3	1.10
6[f]	2	1	70	20	68	39.0	26.4	1.14

[a] **Polymerization conditions:** catalyst: 5 μmol; [ε-CL]/[Y] = 500; toluene = 4 mL. [b] Determined by ^{1}H NMR ($CDCl_3$, RT). [c] Theoretical molecular masses M_n of PCL = 114.14 x ([ε-CL]/[Y-^{i}OPr]) x conversion CL. [d] Molecular masses and their dispersities as determined by GPC (THF, 35°C) vs. polystyrene standards. The M_n GPC values were corrected by 0.56 factor.[14] [e] Catalyst: 2 μmol, [ε-CL]/[Y] = 1000.

View Article Online
DOI: 10.1039/C5DT02938D

Analogous behavior was observed for salalen[16] and salen[17] yttrium complexes, and for dithiaalkanediyl-bridged lanthanide amide complexes.[8a] and was attributed to the dimeric nature of the rare-earth metal alkoxides generated in situ by reaction with the alcohol. At higher temperature (70 °C), in the presence of isopropanol, good conversions were achieved producing polymers whose molecular weights showed a good agreement with the theoretical ones.

The good control over the molecular weights was also confirmed by the linear dependence of the M_n GPC values with the conversion (Figure S10, Supporting Information). When an additional equivalent of alcohol was used, the molecular weights were halved as a consequence of its role as chain transfer agent (run 5, Table 1).

From these observations, we propose that alkoxides generated in situ may exist as a dimer in solution (see next paragraph). In the presence of the monomer, the increase of the temperature favours the cleavage of the dimeric structure and promotes the propagation reaction.

Kinetic studies were performed by monitoring the conversion of ε-caprolactone via ^{1}H NMR spectroscopy. The semilogarithmic plot of $\ln[CL]_0/[CL]_t$ versus time for the polymerization initiated by **1** established a first-order kinetics in monomer concentration (Figure 3).

The performance of the new yttrium complexes **1** and **2** was also explored in the ring-opening polymerization of racemic lactide (Table 2).

Despite the high activity showed in the polymerization of ε-caprolactone, both complexes resulted scarcely reactive toward *rac*-lactide. At room temperature, after 24 h, no conversion was observed.

At 70°C, after the same reaction time, a conversion of only 22% was achieved whereas, after the addition of one equivalent of isopropanol, an almost quantitative conversion was obtained (runs 7 and 8 in Table 2). Kinetic study of LA polymerization initiated by **1** established the first-order kinetics in monomer concentration (Figure 4).

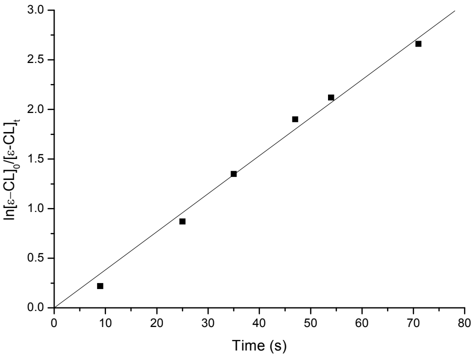

Figure 3. Pseudofirst-order kinetic plot for ROP of ε-CL promoted by **1**. Pseudofirst-order rate constant is (3.83 ± 0.08) 10^{-2} s^{-1} (R = 0,99642). [**1**]= 10 μmol; [ε-CL]/[1] = 500; T = 298 K; toluene = 4 ml as solvent.

View Article Online
DOI: 10.1039/C5DT02238D

Table 2. Polymerization of rac-lactide by catalysts 1-2.[a]

Run	cat	solvent	Conv[b] (%)	$M_{n,th}$[c] (kDa)	M_n,GPC[d,e] (kDa)	M_w/M_n[d]
7	**1**	C_7H_8	92	26.5	15.6	1.39
8	**2**	C_7H_8	68	19.6	11.6	1.44
9	**1**	THF	82	23.7	13.6	1.33
10[f]	**1**	THF	72	20.7	13.0	1.35

[a] **Polymerization conditions:** precatalyst: 10 µmol; ^{i}PrOH: 10 µmol, [*rac*-LA]/[Y]= 200, solvent = 2mL, T = 70 °C, t = 24 h. [b] Determined by ^{1}H NMR ($CDCl_3$, RT). [c] Theoretical molecular masses M_n of PLA (in $gmol^{-1}$) =144.13 x ([L-LA]/[Y-^{i}OPr]) x conversion LA [d] Molecular masses and their dispersities as determined by GPC (THF, 35°C) vs. polystyrene standards. [e] Corrected by 0.58 factor.[14] [f] T = 25 °C, t = 96 h.

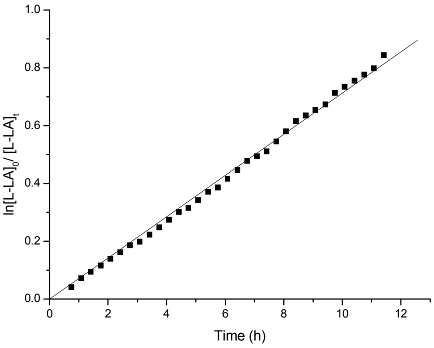

Figure 4. Pseudofirst-order kinetic plot for ROP of *rac*-LA promoted by **1**. Pseudofirst-order rate constant is k_{app} = (7.13 ± 0.04)10^{-2} h^{-1} (R = 0.99915). [**1**]= 0.2 mM; [LA]/[Al]/[^{i}PrOH] = 100:1:1; T = 298 K; toluene-d_8 (0.5 ml) as solvent.

The activity and the degree of control were not significantly dependent on the nature of the solvent: complex **1** showed the same activity in toluene and in THF solution (cfr runs 7 and 9, Table 2).

The molecular weight distributions of the PLAs were unimodal with polydispersity indexes $M_w/M_n \leq 1.44$, but the degree of control over the molar masses was relatively low with M_n values significantly lower than those expected.

The ESI-MS analysis revealed the formation of linear fragments of the type $H\text{-}[OCH(CH_3)C(=O)]_n\text{-}OCH(CH_3)_2$ and $H\text{-}[OCH(CH_3)C(=O)]_n\text{-}OH$ with non integer LA repeat units indicating that intermolecular transesterifications occurred extensively (Figure S11, Supporting Information).

Homodecoupled ^{1}H NMR spectra showed that the PLA samples obtained at 70 °C, both in toluene and THF, had atactic microstructures. A weak heterotactic selectivity, with the probability of racemic linkages between monomer units P_r = 0.72, was observed when the polymerization reaction was performed in THF at room temperature with complex **1** (run 10, Table 2). The stereochemistry of *rac*-lactide enchainment was evaluated by comparing the integrals in the homonuclear decoupled ^{1}H NMR spectrum (Figure S12, Supporting Information), at the tetrad level, with calculated values by using Bernoullian statistics (Table S2, Supporting Information). The good agreement observed confirms that the stereocontrol is due to a chain end control mechanism, whereby the stereo-chemistry of the last inserted LA in the growing chain induces the selection of the incoming enantiomeric monomer.

NMR and DFT studies on the isopropoxo derivative of complex 2

To acquire more insight into the mechanism of the polymerization conducted in the presence of alcohol, the reaction of **2** with isopropanol was monitored by NMR spectroscopy. When **2** was treated with one equivalent of isopropanol in CD_2Cl_2, a rapid evolution of $HN(SiHMe_2)_2$ was observed together with the appearance of a new pattern of resonances attributable to the alkoxo derivative $L^2YOiPr(THF)$ (**2a**). The isopropoxo group replacing the amide group gave rise to a doublet and a multiplet at 1.2 and 4.2 ppm, respectively. The methylene groups $SCH_2\text{-}C(CF_3)_2$ appeared as a sharp singlet slightly highfield shifted compared to that of **2**. ^{1}H NMR monitoring of the reaction showed that the amine elimination is fast and quantitative in few minutes.

It is well known that alkoxo-group 3 metal complexes are prone to aggregation to dimeric/oligomeric structures in which the metal centres are linked by bridging μ^2-alcohoxide groups. To assess the nuclearity of **2a**, diffusion-ordered NMR measurements were performed (CD_2Cl_2, using TMSS as an internal standard). The experimental self-diffusion coefficient of **2a** was 9.83 x 10^{-10} m^2s^{-1} providing a hydrodynamic volume of 704 Å^3. An higher self-diffusion coefficient (11.7 x 10^{-10} m^2s^{-1}) was obtained for the amide precursor **2** which gave a smaller hydrodynamic volume of 502 Å^3 (Figure 5). The larger molecular size observed for **2a** (compared to **2**) suggested a dinuclear solution state structure for **2a**. To propose a molecular geometry and evaluate the relative van der Waals molecular volume, density functional theory (DFT) calculations were performed. The optimized structure of the dimer of **2a** is re-ported in Figure 6, together with the structures of the monomeric alkoxo and amide complexes, i.e. $L^2YOiPr(THF)$ and $L^2YN(SiHMe_2)_2(THF)$. The van der Waals molecular volumes of the dimer and the monomer for the alkoxo complexes were 858 Å^3 and 507 Å^3 respectively.

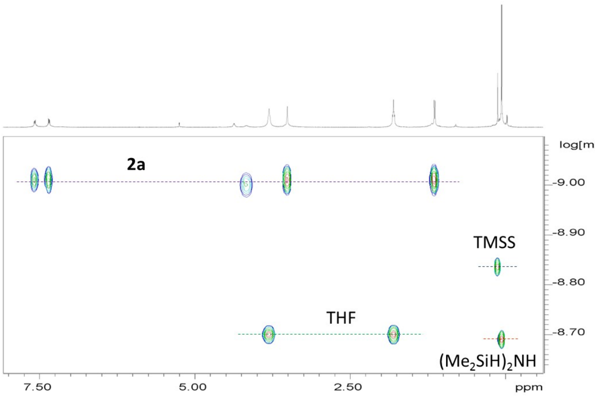

Figure 5. ^{1}H DOSY spectrum of $[L_2YOiPr]_2$ (**2a**) (CD_2Cl_2, rt, 400 MHz)

View Article Online
DOI: 10.1039/C5DT02938D

For comparative purpose the van der Waals molecular volume of the monomeric amide complex **2** was also evaluated (591 Å^3), it was slightly larger than that of the monomeric alkoxo derivative **2a**. The molecular dimensions of **2a** inferred from diffusion NMR data proved to be close to the dimensions of the dimeric species.

The dimerization process was further supported by the theoretical calculation. The calculated free energy change (∆G) for the dimerization reaction, depicted in Scheme 4, indicated that the process is energetically favoured by -14.2 kcal/mol. §§

It is worth noting that in the dimeric structure the yttrium atoms are ligated by two tetradentate OSSO ligands and two bridging μ^2-alkoxides, achieving octahedral environments at each metal centre. Although higher coordination geometries are possible, the THF was not included in the coordination sphere of the metal centre. The absence of a tight interaction between THF and the metal centre was suggested by a close inspection of the DOSY spectrum of **2a** which revealed for the THF a diffusion coefficient different from that observed for **2a** (20.0 x 10^{-10} m^{2}s^{-1}vs 9.83 x 10^{-10} m^{2}s^{-1}, see Figure 5) and close to the value of the free THF (26.5 x 10^{-10} m^{2}s^{-1}). In the case of the monomeric precursor 2, the diffusion coefficient of THF is very close to that of metal complex (14.7 x 10^{-10} m^{2}s^{-1} vs 11.7 x 10^{-10} m^{2}s^{-1}). These values suggest that the THF is reversibly coordinated to the metal centre, according to the following equilibria:

$$L^2YN(SiHMe_2)_2 + THF \leftrightarrow L^2YN(SiHMe_2)_2(THF) \quad (1)$$

$$[L^2YOiPr]_2 + THF \leftrightarrow [L^2YOiPr]_2(THF) \quad (2)$$

Equilibrium 1 results shifted toward the product, whereas equilibrium 2 is shifted toward the reagents.

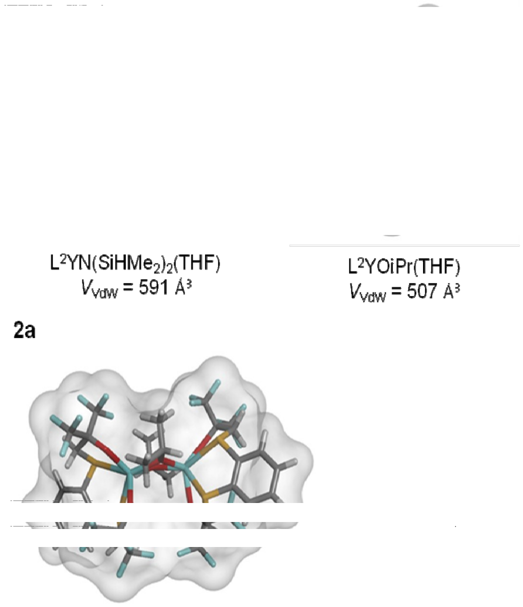

Figure 6. DFT-optimized structures of L^{2}YN(SiHMe$_2$)$_2$(THF) (**2**) L^{2}YOiPr(THF) (**2a'**) and [L^{2}YOiPr]$_2$ (**2a**) with the relative van der Waals molecular volumes.

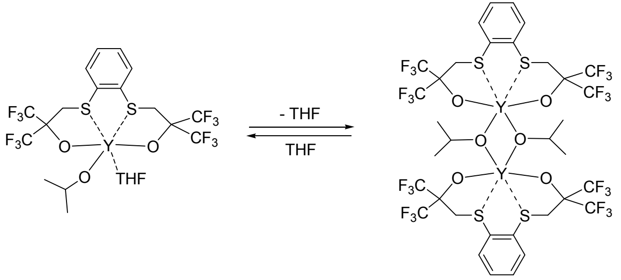

Scheme 4. Formation of the dimeric [L$_2$YOiPr]$_2$ species.

The dimerization process was further supported by the theoretical calculation. The calculated energy change (∆E) for the dimerization reaction, depicted in Scheme 4, indicated that the process is energetically favoured by -2.6 kcal/mol.

ε-Caprolactone Polymerizations by aluminium catalysts 3-4

The aluminium complexes **3** and **4** were tested as initiators in the ROP of ε-CL and *rac*-lactide. Both catalysts resulted inactive toward lactide and showed moderate activities toward ε-CL. The polymerizations of ε-CL were carried out in the presence of one equivalent of iPrOH as activator and the main results are summarized in Table 3. As well-established for aluminium complexes, the reactivity showed by **3** and **4** was much lower than that of parent yttrium complexes and significant polymerization rates were achieved only at 70 °C, with the almost quantitative conversion of 500 equivalents of monomer after six hours (runs 11 and 12, Table 3). At room temperature, the reactivity was notably reduced and quantitative conversions were achieved only after 96 h (run 14, Table 3).

A good control over the molecular weights was observed as evident by the agreement between the experimental number average molecular weight values (M_n) and the theoretical ones calculated as the single-site initiator. This was also confirmed by a series of polymerizations conducted for various monomer to initiator ratios, showing that the number average molecular weight (M_n) increased linearly as the [CL]$_0$/[Al]$_0$ ratio was increased (Figure S13, Supporting Information).

Table 3. Polymerization of ε-caprolactone by catalysts 3-4.[a]

Run	cat.	[ε-CL]/[Al]	Conv[b] (%)	$M_{n,th}$[c] (kDa)	$M_{n,GPC}$[d,e] (kDa)	M_w/M_n[d]
11	3	500	94	53.3	56.3	1.15
12	4	500	80	45.6	50.2	1.66
13	4	25	98	3.5	3.1	1.14
14[e]	4	500	95	54.2	45.9	1.47

[a] **Polymerization conditions:** precatalyst: 10 μmol; ^{i}PrOH: 10 μmol; 10 μL of a 0.1 M toluene solution; toluene: 2 mL, T = 70 °C, t = 6 h. [b] Determined by ^{1}H NMR (CDCl$_3$, RT). [c] Theoretical molecular masses. [d] Molecular masses and their dispersities as determined by GPC (THF, 35°C) vs. polystyrene standards and corrected by 0.56 factor.[14] [e] T = 25 °C, t = 96 h.

View Article Online
DOI: 10.1039/C5DT02938D

The initiation mechanism was elucidated by end-group analysis. The ^{1}H NMR spectrum (Figure 7) of a low molecular weight chain (run 13, Table 3) clearly showed the presence of isopropoxo group according to the resonances at 1.25 and 5.05 ppm, as a consequence of the exchange reaction of 2-propanol with the methyl group at the aluminium centre.

Kinetic studies of ε-CL polymerization established the first-order kinetics in monomer concentration at different temperatures (Figure 8). The relationship between ln k_{app} and the reciprocal of polymerization temperature (1/T) is shown in Figure 9. According to the Arrhenius equation, the activation energy calculated for **4**/ iPrOH is E_a= 67.8 kJ mol^{-1}.

This value is quite high, coherently with the moderate activities observed, however it is comparable with those observed for other aluminium complexes bearing two monoanionic phenolate ligands.[18]

Experimental

Materials and methods

All manipulations of air- and/or water-sensitive compounds were carried out under a dry nitrogen atmosphere using a Braun Labmaster glove box or standard Schlenk-line techniques. Glassware and vials used in the polymerization were dried in an oven at 120 °C overnight and exposed to vacuum-nitrogen cycles thrice.

Benzene, hexane, THF and toluene were distilled over sodium benzophenone. $CDCl_3$, CD_2Cl_2, and C_6D_6 were dried using molecular sieves. Lactide was purified by crystallization from dry toluene. ^{i}PrOH was purified by distillation over sodium. ε-CL was dried with CaH_2 for 24 h at room temperature and then distilled under reduced pressure. All other chemicals were commercially available and used as received unless otherwise stated. Yttrium precursor and ligands L^1-H_2 and L^2-H_2 were prepared according to published procedures.[10,19]

Elemental analyses were performed in the microanalytical laboratory of the Department of Chemistry and Biology.

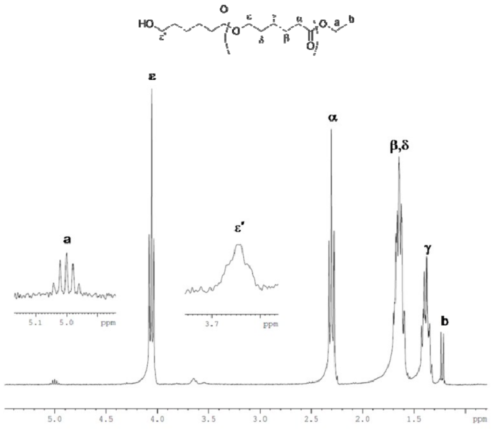

Figure 7. ^{1}H NMR (300 MHz, $CDCl_3$, RT) spectrum of a low molecular weight poly(ε-caprolactone) by catalyst **4** (Table 3, run 13).

Figure 8. Kinetic plots for ROP of ε-CL promoted by **4** + ^{i}PrOH at different temperatures.

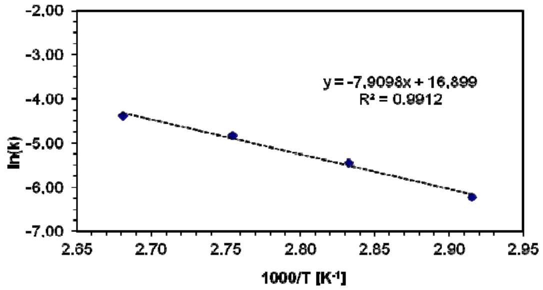

Figure 9. Arrhenius plot for ROP of ε-CL promoted by **4** + ^{i}PrOH.

NMR spectra of complexes and polymers were recorded on Bruker Avance spectrometers; resonances are reported in ppm (δ) and the coupling constants in Hz (*J*), and are referenced to the residual solvent peak versus $Si(CH_3)_4$: at δ 7.26 (^{1}H) δ 77.16 (^{13}C); in the case of 19F, resonances were automatically referenced versus $CF_3C_6H_5$ by the software. J.Young NMR tubes were employed for the spectra of complexes and complexes reactivity.

Molecular masses (M_n and M_w) and their dispersities (M_w/M_n) were measured by gel permeation chromatography (GPC). The measurements were performed at 30 °C on a Waters 1525 binary system equipped with a Waters 2414 Refractive Index (RI) detector; using THF as eluent (1.0 mL min^{-1}) and employing a system of four Styragel HR columns (7.8 x 300 mm; range 10^3 – 10^6 Å). Narrow polystyrene standards were used as reference and Waters Breeze v3.30 software for data processing.

Crystallography

X-ray diffraction quality single crystals of **2** were obtained as yellow prisms from hexane solutions at 253 K. A suitable crystal (0.46 mm x 0.39 mm x 0.30 mm) was selected and mounted on a cryoloop with Paratone® N and measured at 100 K with a Rigaku AFC7S diffractometer equipped with a Mercury^2 CCD detector using graphite monochromated Mo$K\alpha$ radiation (λ = 0.71069 Å). Data reduction was performed with the crystallographic package CrystalClear.[20] Data have been corrected for Lorentz, polarization and absorption. The structure was solved by direct methods using the program SIR2002[21] and refined by means of full matrix least-squares based on F^2 using the program SHELXL97.[22] For all compounds non-hydrogen atoms were refined anisotropically, hydrogen atoms were positioned geometrically and included in structure factors calculations but not refined. 389 refinable parameters were finally considered, final disagreement indices are R = 0.0851 (5135 reflections F^2>2σF^2), $_w$R2= 0.2440 (all 6894 independent reflections). Maximum and minimum residual density were respectively +1.874 and -1.17 e Å^{-3}. Crystal structures were drawn using Mercury.[23]

Synthetic procedures

Synthesis of complex L^{1}YNR$_2$ (1). A solution of ligand L^1-H$_2$ (150 mg, 0.330 mmol) in benzene (5.5 mL) was added dropwise to a solution of [Y(N(SiMe$_2$H)$_2$)$_3$](THF)$_2$ (208 mg, 0.330 mmol) in benzene (5.0 mL). The reaction mixture was stirred for 1 h at room temperature, then the solvent was removed. The obtained solid was dissolved in *n*-hexane (1 mL) and dried in vacuum to yield a white powder. Yield: 92 %.

Elemental analysis calcd (%) for $C_{18}H_{30}F_{12}NO_3S_2Si_2Y$: C, 28.99; H, 4.06; N, 1.88; S, 8.60. Found: C, 28.82; H, 4.13; N, 1.83; S, 8.67

δ_H (300 MHz, C_6D_6, RT) 4.94 (2H, br s, SiH), 3.90 (4H, br s, OCH$_2$), 2.80 (4H, br s, SCH$_2$C(O)(CF$_3$)$_2$), 1.98 (4H, br s, SCH$_2$CH$_2$S), 1.24 (4H, br s, OCH$_2$*C*H$_2$), 0.36 (12H, d, J_{HH} 3.0, SiH(C*H*$_3$)$_2$).

δ_C (75.5 MHz, C_6D_6, RT) 126.95 (4C, q, $^1J_{CF}$ 290.3, CF$_3$), 82.7 (2C, m, *C*(CF$_3$)$_2$), 71.1 (2C, s, OCH$_2$), 39.45 (2C, s, S*C*H$_2$C(O)(CF$_3$)$_2$), 33.45 (2C, s, SCH$_2$CH$_2$S), 25.15 (2C, s, OCH$_2$*C*H$_2$), 3.2 (4C, s, SiH(*C*H$_3$)$_2$).

δ_F (376.5 MHz, C_6D_6, RT) -78.9 (12F, s, CF$_3$).

Synthesis of complex L^{2}YNR$_2$ (2). A solution of ligand L^2-H$_2$ (150 mg, 0.330 mmol) in benzene (5.5 mL) was added dropwise to a solution of [Y(N(SiMe$_2$H)$_2$)$_3$](THF)$_2$ (188 mg, 0.298 mmol) in benzene (5.0 mL). The reaction mixture was stirred for 1 h at room temperature, then concentrated at reduced pressure. The obtained solid was dissolved in *n*-hexane (1 mL) and dried in vacuum to yield a white powder. Yield: 89 %.

Elemental analysis calcd (%) for $C_{22}H_{30}F_{12}NO_3S_2Si_2Y$: C, 33.29; H, 3.81; N, 1.76; S, 8.08. Found: C, 33.97; H, 3.77; N, 1.66; S, 8.12.

δ_H (400 MHz, C_6D_6, RT) 6.90–6.85 (2H, m, Ar-H), 6.75–6.67 (2H, m, Ar-H), 4.76 (2H, br s, SiH), 3.93 (4H, m, OCH$_2$), 3.40 (4H, br s, SCH$_2$), 1.31 (4H, br s, OCH$_2$C*H*$_2$), 0.29 (12H, d, J_{HH} 2.7, SiH(C*H*$_3$)$_2$).

δ_C (62.9 MHz, C_6D_6, RT) 137.55 (2C, s, ArC-S), 134.0 (2C, s, ArC-H); 130.1 (2C, s, ArC-H); 125.3 (4C, q, $^1J_{CF}$ 291.3, CF$_3$), 82.5 (2C, septuplet, $^2J_{CF}$ 28.5 Hz, *C*(CF$_3$)$_2$), 71.0 (2C, s, OCH$_2$), 44.15 (2C, s, S*C*H$_2$C(O)(CF$_3$)$_2$), 25.65 (2C, s, SCH$_2$CH$_2$S), 3.22 (4C, s, SiH(*C*H$_3$)$_2$).

δ_F (376.5 MHz, C_6D_6, RT) -77.9 (12F, br s, CF$_3$).

Crystallographic data of **2:** Molecular formula $YC_{22}H_{30}F_{12}NO_3S_2Si_2$, MW 793.68, triclinic, P-1, a = 10.584(9) Å, b = 10.661(9) Å, c = 14.958(11) Å, α = 91.476(18)°, β = 95.111(19)°, γ = 104.21(3)°, V=1628(2) Å^3, Z = 2, D_c = 1.619 g/cm^3, F(000) = 800, μ = 2.088 mm^{-1}.

Synthesis of complex L^{1}AlMe (3). A solution of AlMe$_3$ (30 mg, 0.416 mmol) in benzene (1 mL) was added dropwise to a solution of L^1-H$_2$ (189 mg, 0.416 mmol) in benzene (4 mL). The reaction mixture was stirred for 30 min at room temperature, then concentrated at reduced pressure. The obtained solid was dissolved in *n*-pentane (1 mL) and dried in vacuum to yield a white powder. Yield: 73 %

Elemental analysis calcd (%) for $C_{11}H_{11}AlF_{12}O_2S_2$: C, 26.73; H, 2.24; S, 12.97. Found: C, 26.61; H, 2.17; S, 13.06.

δ_H (400 MHz, C_6D_6, RT) 3.15-2.00 (4H, br m, SCH$_2$CH$_2$S), 1.66 (4H, br s, SCH$_2$C(O)(CF$_3$)$_2$), -0.13 (3H, br s, Al-CH$_3$).

δ_c NMR (62.9 MHz, C_6D_6, RT) 124.4 (4C, q, $^1J_{CF}$ 289.2, CF$_3$), 77.55 (2C, septuplet, $^2J_{CF}$ 29.4 Hz, *C*(CF$_3$)$_2$), 38.0 (2H, s, S*C*H$_2$C(O)(CF$_3$)$_2$), 34.75 (2C, s, SCH$_2$CH$_2$S), -11.7 (1C, br s, Al-CH$_3$).

δ_F (376.5 MHz, C_6D_6, RT) -78.2 (12F, br s, CF$_3$).

Synthesis of complex L^{2}AlMe (4). A solution of ligand L^2-H$_2$ (100 mg, 0.199 mmol) in benzene (2.0 mL) was added dropwise to a solution of AlMe$_3$ (14.8 mg, 0.205 mmol) in benzene (2.5 mL). The reaction mixture was stirred for 1 h at room temperature, then concentrated at reduced pressure. The obtained solid was dissolved in *n*-hexane and dried in vacuum to yield a white powder. Yield: 87 %.

Elemental analysis calcd (%) for $C_{15}H_{11}AlF_{12}O_2S_2$: C, 33.22; H, 2.04; S, 11.82. Found: C, 33.35; H, 2.16; S, 11.94.

δ_H (400 MHz, C_6D_6, RT) 6.70–6.60 (2H, m, Ar-H), 6.60–6.50 (2H, m, Ar-H), 3.29 (2H, d, $^2J_{HaHb}$ 14.2, SCH$_2$), 3.04 (2H, d, $^2J_{HaHb}$ 14.2, SCH$_2$), -0.08 (3H, s, Al-CH$_3$).

δ_C (62.9 MHz, C_6D_6, RT) 134.5 (2C, s, ArC-S), 132.5 (2C, s, ArC-H), 130.7 (2C, s, ArC-H), 123.8 (4C, 2q, $^1J_{CF}$ 289.8, CF$_3$), 77.1 (2C, septuplet, $^2J_{CF}$ 30.1, *C*(CF$_3$)$_2$), 43.1 (2C, s, S-CH$_2$), -11.0 (1C, br s, Al-CH$_3$).

δ_F (376.5 MHz, C_6D_6, RT)-78.25 (6F, q, $^4J_{FF}$ 8.5, CF$_3$), -78.4 (6F, q, $^4J_{FF}$ 8.5, CF$_3$).

Polymerization reactions

ε-Caprolactone polymerizations by catalysts 1-2. In a typical experiment (Table 1, run 1), in glovebox, a 4 mL vial was sequentially charged with a solution of catalyst (5 µmol) in toluene (1 mL), a solution of ε-caprolactone (2.5 mmol) in toluene (1 mL). The reaction mixture was stirred for the desired time and then quenched by adding wet *n*-hexane. Precipitated solid was filtered and dried in a vacuum oven overnight at 40 °C.

***rac*-Lactide polymerizations by catalysts 1-2.** In a typical experiment (Table 2, run 2), in glovebox, a 10 mL Schlenk tube was sequentially charged with *rac*-lactide (2.0 mmol), toluene (1 mL), a solution of catalyst (10 µmol) and isopropanol (10 µmol, 100 µL of a 0.1 M toluene solution) in toluene (1 mL). The tube was put in an oil bath, preheated and thermostated at 70 °C. The reaction mixture was stirred for the desired time and then quenched by adding wet *n*-hexane. Precipitated solid was filtered and dried in a vacuum oven overnight at 40 °C.

ε-Caprolactone polymerizations by catalysts 3-4. In a typical experiment (Table 2, run 1), in glovebox, a 10 mL Schlenk tube was sequentially charged with a solution of ε-caprolactone (5.0 mmol) in toluene (1 mL), a solution of catalyst (10 µmol) and isopropanol (10 µmol, 100 µL of a 0.1 M toluene solution) in toluene (1 mL). The tube was put in an oil bath, preheated and thermostated at 70 °C. The reaction mixture was stirred for the desired time and then quenched by adding wet *n*-hexane. Precipitated solid was filtered and dried in a vacuum oven overnight at 40 °C.

Kinetic studies. In a typical experiment, in glovebox, a J.Young NMR tube was sequentially charged with a solution of catalyst

(5 µmol) in toluene-d_8 (0.1 mL), isopropanol (5 µmol, 50 µL of a 0.1 M toluene solution), monomer (1.00 mmol, 200 equiv), 0.4 mL of toluene-d_8 to adjust the total volume to 0.5 mL. The NMR tube was placed into the NMR Bruker spectrometer, preheated and thermostated at the desired temperature, and the multi_zgvd (variable delay) function was employed to record spectra at fixed intervals of time. Conversion values were calculated from polymer and monomer integrals, and the spectrum recording time was taken into account for the kinetic plot.

Investigation on catalytic species

Synthesis of complex L2YOiPr(THF) (2a). *(NMR Tube Reaction)* In a glovebox, isopropanol (1.1 µL, 0.015 mmol) dissolved in CD_2Cl_2 (0.3 mL) was added to a solution of complex **2** (11.5 mg, 0.015 mmol) in CD_2Cl_2 (0.3 mL) at room temperature. The resulting pale yellow solution was transferred to a NMR tube and analyzed.

δ_H (400 MHz, CD_2Cl_2, RT) 7.64 (2H, m, Ar-H), 7.41 (2H, m, Ar-H), 4.25 (1H, m, $OCH(CH_3)_2$), 3.88 (4H, br s, OCH_2), 3.59 (4H, br s, SCH_2), 1.88 (4H, m, OCH_2CH_2), 1.22 (6H, d, $OCH(CH_3)_2$).

DOSY experiments. The measurement of diffusion has been carried out by observing the attenuation of the NMR signals during a pulsed field gradient experiment using the double stimulated echo pulse sequence.[20] In particular, 2D DOSY PGSE NMR spectra were performed on a Bruker Avance 400 spectrometer at 298 K without spinning. Tetrakistrimethylsilylsilane (TMSS) was added as the internal standard. The parameters δ and Δ were kept constant during the experiments, whereas G varied from 2 to 95% in 32 steps. The value of δ was 500 µs. (see Supporting Information for further details). The diffusion coefficients remained substantial unchanged over the range of concentration 30 - 3 mM.

Computational details. Density functional theory (DFT) calculations were performed with the program suite Gaussian 09.[21] All geometries were optimization without constraints at the BP86 level, i.e., employing the exchange and correlation functionals of Becke and Perdew,[22] respectively. The basis set consisted of the Los Alamos basis sets and corresponding effective core potentials of Hay and Wadt[23] (LANL2DZ) for Y and of the 6-31G(d) basis sets for all other atoms. Geometry optimizations were performed without symmetry constraints. Stationary point geometries were characterized as local minimum on the potential energy surfaces. The absence of imaginary frequency verified that structures were true minima at their respective levels of theory. The van der Waals volumes were obtained from the DFT optimized structures using the software package Discovery Studio 4.1 Visualizer.

Conclusions

Two new yttrium and two new aluminium complexes, bearing dithiodiolate ligands, have been synthesized, fully characterized and tested as initiators in the ring-opening polymerization of ε-CL and *rac*-LA. Yttrium complexes promoted controlled polymerization of ε-CL and *rac*-LA in the presence of isopropyl alcohol, whereas in the absence of the alcohol these complexes resulted highly active in the production of high mo-lecular weight PCLs. DOSY experiments and DFT calculations suggested the formation of a dimeric structure for the isopropoxo derivative in which the yttrium atoms result bound to two tetradentate OSSO ligands and two bridging μ^2-alkoxides while the monomeric species is favoured for the yt-trium amide complex. The different steric encumberance of the metal centres in the two discussed species could explain the lower activities of the isopropoxo species with respect to the amide species in the polymerization reactions.

Aluminium complexes showed moderate activities toward ε-CL while resulted inactive with respect to *rac*-lactide.

Acknowledgements

The authors thank Moshe Kol (Tel Aviv University) for useful discussion, Dr. Ilaria D'Auria for GPC measurements, Dr. Patrizia Iannece for elemental analysis and Dr. Patrizia Oliva for NMR technical assistance. This work was supported by the Italian Ministry of University and Research (PRIN 2010–2011: nanostructured polymeric materials with tailored molecular and crystalline structures, for advanced technologies and for the environment)

Notes and references

‡ Indeed in this case the H atom bonded to Si1 atom could be located in the difference Fourier map (at difference with the H atom bonded to the Si2 atom).

§ For similar complexes, some authors[12] invoked the formation of pentacoordinate species by dissociation of the THF. In our case we rule out this possibility taking into account both the chemical shift of the THF in the ^{1}H NMR and the DOSY experiment results (vide infra).

§§ DFT calculations indicated that the rupture of the dimer by CL or LA is not energetically favoured.

1 (*a*) R. H. Platel, L. M. Hodgson and C. K. Williams, *Polym. Rev.*, 2008, **48**, 11; (*b*) B. J. O'Keefe, M. A. Hillmyer and W. B. Tolman, *J. Chem. Soc., Dalton Trans.*, 2001, 2215; (*c*) A. Arbaoui and C. Redshaw, *Polym. Chem.* 2010, **1**, 801.

2 A.-C. Albertsson and I. K. Varma, *Biomacromolecules*, 2003, **4**, 1466.

3 A. Amgoune, C. M. Thomas and J. F. Carpentier, *Pure Appl. Chem.* 2007, **79**, 2013.

4 (*a*) J. Wu, T. -L. Yu, C. -T. Chen and C. -C. Lin, *Coord. Chem. Rev.* 2006, **250**, 602; (*b*) P. Hormniurun, E. D. Marshall, V. C. Gibson, R. I. Pugh and A. J. P. White, *Proc. Natl. Acad. Sci. U.S.A.* 2006, **42**, 15343.

5 (*a*) C. M. Thomas, *Chem. Soc. Rev.*, 2010, **39**, 165; (*b*) M. J. Stanford and A. P. Dove, *Chem. Soc. Rev.*, 2010, **39**, 486; (c) P. J. Dijkstra, H. Du and J. Feijen, *Polym. Chem.*, 2011, **2**, 520; (*d*) S. Slomkowski, S. Penczek and A. Duda, *Polym. Adv. Technol.*, 2014, **25**, 436; (*e*) N. Spassky, M. Wisniewski, C. Pluta and A. Le Borgne, *Makromol. Chem. Phys.*, 1996, **197**, 2627; (*f*) N. Nomura, R. Ishii, Y. Yamamoto and T. Kondo, *Chem. Eur. J.*, 2007, **13**, 4433; (*g*) A. Pilone, K. Press, I. Goldberg, M. Kol, M. Mazzeo and M. Lamberti, *J. Am. Chem. Soc.*, 2014, **136**, 2940.

6 (*a*) M. P. Coles, D. C. Swenson, R. F. Jordan, V. G. Young, *Organometallics*, 1998, **17**, 4042; (*b*) B. Lian, H. Ma, T. P. Spaniol and J. Okuda, *Dalton Trans.*, 2009, 9033; (*c*) M. Lamberti, I. D'Auria, M. Mazzeo, S. Milione, V. Bertolasi and D. Pappalardo, *Organometallics*, 2012, **31**, 5551; (*d*) L.

Postigo, M. D. C. Maestre, M. E. G. Mosquera, T. Cuenca, G. Jimenez, *Organometallics*, 2013, **32**, 2618; (*e*) F. Della Monica, E. Luciano, G. Roviello, A. Grassi, S. Milione and C. Capacchione, *Macromolecules*, 2014, **47**, 2830.

7 (*a*) A. Amgoune, L. Lavanant, C. M. Thomas, Y. Chi, R. Welter, S. Dagorne and J.-F. Carpentier, *Organometallics*, 2005, **24**, 6279; (*b*) M. Bouyahi, E. Grunova, N. Marquet, E. Kirillov, C. M. Thomas, T. Roisnel, J.-F. Carpentier, *Organometallics*, 2008, **27**, 5815; (*c*) A. Alaaeddine, C. M. Thomas, T. Roisnel, J.-F. Carpentier, *Organometallics*, 2009, **28**, 1469; (*d*) M. Bouyahyi, T. Roisnel and J.-F- Carpentier, *Organometallics*, 2012, **31**, 1458; (*e*) N. Maudoux, T. Roisnel, J.-F. Carpentier and Y. Sarazin, *Organometallics*, 2014, **33**, 5740; (*f*) Third group complexes bearing the same class of ligands were also reported: E. Grunova, E. Kirillov, T. Roisnel and J.-F. Carpentier, *Organometallics*, 2008, **27**, 5691.

8 (*a*) H. Ma, T. P. Spaniol and J. Okuda, *Angew. Chem., Int. Ed.*, 2006, **45**, 7818; (b) H. Ma, T. P. Spaniol and J. Okuda, *Inorg. Chem.*, 2008, **47**, 3328; (*c*) J.-C. Buffet, A. Kapelski and J. Okuda, *Macromolecules*, 2010, **43**, 10201; (*d*) Aluminium complexes bearing the same class of ligands were also reported: H. Ma, G. Melillo, L. Oliva, T. P. Spaniol, U. Englert and Okuda, *Dalton Trans.*, 2005, 721.

9 (*a*) M. Mazzeo, R. Tramontano, M. Lamberti, A. Pilone, S. Milione, C. Pellecchia, *Dalton Trans.* 2013, **42**, 9338; (*b*) A. Pilone, M. Lamberti, M. Mazzeo, S. Milione and C. Pellecchia, *Dalton Trans.* 2013, **42**, 13036.

10 E. Sergeeva, J. Kopilov, I. Goldberg and M. Kol, *Inorg. Chem.*, 2010, **49**, 3977.

11 O. Runte, T. Priermeiera and R. Anwander, *Chem. Commun.*, 1996, 1385.

12 H. Ma, T. P. Spaniol, J. Okuda, *Dalton Trans.*, 2003, 4770.

13 L. Lavanant, T.-Y. Chou, Y. Chi, C. W. Lehmann, L. Toupet and J.-F. Carpentier, *Organometallics*, 2004, **23**, 5450.

14 M. Save, M. Schappacher, A. Soum, *Macromol. Chem. Phys.*, 2002, **203**, 889.

15 M. Cheng, A. B. Attygalle, E. B. Lobkovsky and G. W. Coates, *J. Am. Chem. Soc.*, 1999, **121**, 11583.

16 K. Nie, W. Gu, Y. Yao, Y. Zhang and Q. Shen, *Organometallics*, 2013, **32**, 2608.

17 W. Gu, P. Xu, Y. Wang, Y. Yao, D. Yuan and Q. Shen, *Organometallics*, 2015, **34**, 2907.

18 N. Ikpo, M. S. Barbon, M. W. Drover, L. N. Dawe and F. M. Kerton, *Organometallics*, 2012, **31**, 8145.

19 W. A. Herrmann, F. C. Munck, G. R. J. Artus, O. Runte and R. Anwander, *Organometallics*, 1997, **16**, 682.

20 CrystalClear, Crystal Structure Analysis Package, Rigaku-Molecular Structure Corp.

21 M. C. Burla, M. Camalli, B. Carrozzini, G. L. Cascarano, C. Giacovazzo, G. Polidori and R. Spagna, *J. Appl. Cryst.*, 2003, **36**, 1103.

22 G. M. Sheldrick, *Acta Cryst.*, 2008, **A64**, 112.

23 C. F. Macrae, I. J. Bruno, J. A. Chisholm, P. R. Edgington, P. McCabe, E. Pidcock, L. Rodriguez-Monge, R. Taylor, J. van de Streek and P. A. Wood, *J. Appl. Cryst.*, 2008, **41**, 466.

24 (*a*) A. Jerschow and N. Muller, *J. Magn. Reson.*, 1997, **125**, 372; (*b*) A. A. Khrapitchev and P. T. Callaghan, *J. Magn. Reson.*, 2001, **152**, 259.

25 M. J. Frisch, G. W. Trucks, H. B. Schlegel, G. E. Scuseria, M. A. Robb, J. R. Cheeseman, G. Scalmani, V. Barone, B. Mennucci, G. A. Petersson, H. Nakatsuji, M. Caricato, X. Li, H. P. Hratchian, A. F. Izmaylov, J. Bloino, G. Zheng, J. L. Sonnenberg, M. Hada, M. Ehara, K. Toyota, R. Fukuda, J. Hasegawa, M. Ishida, T. Nakajima, Y. Honda, O. Kitao, H. Nakai, T. Vreven, J. A. Montgomery, Jr., J. E. Peralta, F. Ogliaro, M. Bearpark, J. J. Heyd, E. Brothers, K. N. Kudin, V. N. Staroverov, R. Kobayashi, J. Normand, K. Raghavachari, A. Rendell, J. C. Burant, S. S. Iyengar, J. Tomasi, M. Cossi, N. Rega, J. M. Millam, M. Klene, J. E. Knox, J. B. Cross, V. Bakken, C. Adamo, J. Jaramillo, R. Gomperts, R. E. Stratmann, O. Yazyev, A. J. Austin, R. Cammi, C. Pomelli, J. W. Ochterski, R. L. Martin, K. Morokuma, V. G. Zakrzewski, G. A. Voth, P. Salvador, J. J. Dannenberg, S. Dapprich, A. D. Daniels, Ö. Farkas, J. B. Foresman, J. V. Ortiz, J. Cioslowski, and D. J. Fox, Gaussian 09, revision A.02; Gaussian, Inc.: Wallingford, CT, 2009.

26 (*a*) A. D. Becke, *Phys. Rev. A*, 1988, **38**, 3098; (*b*) J. P. Perdew, *Phys. Rev. B*, 1986, **33**, 8822; (**c**) J. P. Perdew, *Phys. Rev. B*, 1986, **34**, 7406.

27 (*a*) P. J. Hay and W. R. Wadt, *J. Chem. Phys.*, 1985, **82**, 270; (*b*) W. R. Wadt and P. J. Hay, *J. Chem. Phys.*, 1985, **8**2, 284.